Salt Effects on the Structure and Dynamics of Interfacial Water on Calcite Probed by Equilibrium Molecular Dynamics Simulations

Azeezat Ali, Tran Thi Bao Le and Alberto Striolo*
Department of Chemical Engineering, University College London, London WC1E 6BT United Kingdom

David R. Cole
School of Earth Sciences, The Ohio State University, Columbus, Ohio 43210 United States of America

ABSTRACT

It is important to understand the properties of interfacial water at mineral surfaces. Since calcite is one of the most common minerals found in rocks and sedimentary deposits, and since it represents a likely phase encountered in reservoirs dedicated to carbon sequestration, it is crucial to understand the behaviour of fluids on its surface. In this study, the impacts of sodium chloride (NaCl), potassium chloride (KCl) and magnesium chloride ($MgCl_2$) on the structure and dynamics of water on the calcite interface were investigated using equilibrium molecular dynamics simulations. Two force fields were compared to model calcite. The resultant properties of interfacial water were quantified and compared in terms of atomic density profiles, surface density distributions, radial distribution functions, hydrogen bond density profiles, angular distributions, and residence times. Our results show the formation of distinct interfacial molecular layers, with water molecules in each layer having slightly different orientations, depending on the force field implemented. The fluid behaviour within the first interfacial layers differs from that observed in bulk water. There was a tendency for water molecules in adjacent layers to form hydrogen bonds between each other or the surface, as opposed to the formation of hydrogen bonds within each hydration layer. The addition of ions disrupts the well-organized structure of oxygen atoms in the first and second hydration layers, with KCl having the biggest effect. Conversely, far from the interface, $MgCl_2$ leads to the lowest number of hydrogen bonds per water, out of the salts considered. The residence time of water within the second hydration layer follows a bi-exponential decay, suggesting the simultaneous presence of two dynamic mechanisms, one characterized by shorter time scales than the other. The time scale associated with the former mechanism decreases as the salt concentration is increased, whereas the opposite is observed for the slower mechanism. In general, the results obtained with the two force fields used to simulate calcite are similar in terms of the features of the hydration layers and hydrogen bond network but differ significantly in their predictions for the residence times. Although experimental results are not available to identify which of the two force fields yields predictions that more closely resemble reality, the results highlight the contributions of surface-water, water-water, and ion-water interactions on the wetting properties of calcite, which are especially important for calcite-water-electrolyte interactions commonly observed in nature.

* Corresponding Author: a.striolo@ucl.ac.uk

1. INTRODUCTION

The properties of interfacial fluids are of great importance in a wide range of biological and chemical processes. In the energy industry, for example, such properties play a crucial role in nuclear waste storage, CO_2 sequestration, and enhanced oil recovery, as they relate to interfacial tension, wettability alterations, and interfacial mass transfer of CO_2, water and oil mixtures. Because these properties govern fluid distribution and behaviour in porous media, they control the capillary sealing efficiency, with respect to CO_2, of the cap rock as well as the transport properties of water, brine and CO_2 phases.[1-3] Because water-wet reservoirs yield higher oil recovery than oil-wet reservoirs,[4] the study of interfacial fluids on mineral substrates could enable the identification of conditions in which reservoirs are attractive for exploitation.

The effects of ions on the bulk properties of water have been widely researched. It has been shown that ions generally lead to changes in the bulk water properties, such as the hydrogen bonding network, with different ions having varying effects.[5-8] The structure of water in salt solutions is the result of subtle balances between electrostatic and dispersive interactions, mediated by the ability of water molecules to form hydrogen bonds. Ions have been classified as kosmotropes and chaotropes based on their perceived ability to promote or disrupt the order among water molecules, respectively.[9,10] For example, Conte[11] found, through NMR relaxometry measurements, that NaCl, $CaCl_2$, and KCO_3 are kosmotropes, while KCl is a chaotrope. Nag et al.[12] and Riemenschneider et al.[13] conducted molecular dynamics simulations for NaCl and CsCl in water. They found a replacement of water-water hydrogen bonds with ion-water interactions in aqueous NaCl,[12,13] while CsCl enhanced the water hydrogen bond network.[13] Neutron diffraction and Raman experimental studies showed that the effects of ions on the structure of water is equivalent to the effects of high pressures, in terms of the distortion of hydrogen bonds through the fluids.[5] Through a detailed comparison of experimental Raman spectral measurements with classical Monte Carlo (MC) simulations, Smith et al.[6] reported that anions exert electric fields on the adjacent hydrogen atoms of water molecules as opposed to structural rearrangements in the hydrogen-bond network.[6] Ions have also been shown to sometimes accelerate, as well as slow down the water dynamics, depending on experimental conditions.[8] For example, NMR measurements revealed that Na^+ ions have a retarding effect on water, while K^+ ions accelerate water dynamics.[14] It would be of interest to quantify how these phenomena are affected by the proximity to a solid surface.

One of the most abundant minerals found on earth is calcium carbonate ($CaCO_3$), with calcite being the most common (approximately 4% of the Earth's crust consists of calcite). Calcite is an anhydrous calcium carbonate polymorph.[15] Many conventional hydrocarbon reservoirs are also based on calcium carbonate, and such reservoirs have been considered as potential engineered reservoirs for carbon sequestration. Because interactions between calcite and water relate to the wettability of this mineral, it is essential to understand the interfacial water structure on calcite, as well as how it is affected by salt ions. Such results could also help to constrain the effects of salts on confined fluids from a fundamental point of view.

Several molecular dynamics studies carried out on interfacial water on mineral substrates such as alumina,[16] silica,[17,18] quartz[19,20] mica,[21,22] and calcite,[23-29] found that the structural and dynamical properties of interfacial water depend on the properties of the mineral substrate, and in general they differ from properties observed in bulk water. Such studies are in some cases

supported by experimental observations, as was the case for Fenter et al.,[23,24,28] who included experimental X-ray reflectivity data in their study on calcite. There have also been molecular dynamics studies on the effects of ions in aqueous solutions on interfaces. Ho et al.[30] and Argyris et al.[31] compared the behaviour of aqueous NaCl and CsCl confined in narrow silica pores. These studies focused on the transport properties of water and ions, which depend on the cation type and degree of protonation of silica. Ma et al.[32] conducted a study on aqueous Na_2SO_4 confined in quartz pores, and found through atomic and radial density profiles that there are stronger interactions between Na^+ ions and water with the surface than with SO_4^{2-}. Dello Stritto et al.[33,34] studied the effects of Na^+, Rb^+, Mg^{2+} and Sr^{2+} ions on the hydrogen bond structure and dynamics of quartz-water interface and reported that divalent cations adsorb more strongly than monovalent ions at this surface. They also found that the cation type determines the degree of ordering of interfacial water with the ions promoting intra-surface hydrogen bonding. Kerisit et al.[35] investigated the adsorption of NaCl, CsCl and CsF on neutral goethite. They reported strong adsorption of water on the surface and noted the influence of the ions size on the location and extent of adsorption, which determines the rearrangement of interfacial water. Simonnin et al.[36] studied the clay-water interface in the presence of NaCl and CsCl ions; they found that structure, diffusion, and hydrodynamic properties of aqueous solutions on clay depend on the nature of the clay, the nature of the counter ions, and the salt concentration.

Predota et al.[37,38] investigated, through molecular dynamics studies and X-ray reflectivity experiments, the effects of Rb^+, Na^+, Sr^{2+}, Zn^{2+}, Ca^{2+}, and Cl^- ions on the structure of interfacial water on rutile (TiO_2) surface. They found that the structure of interfacial water is independent of the cations but dependent on the surface charge. They reported the formation of inner-sphere complexes of cations with surface oxygens for all cations studied, although the preferential adsorption sites varied according to the cations' ionic radius. These results are consistent with the studies by Zhang et al.,[39-41] who applied X-ray reflectivity, X-ray standing wave measurements, and Density Functional Theory (DFT), in addition to molecular dynamics simulations, to study the adsorption of ions (Na^+, Rb^+, Ca^{2+}, Sr^{2+}, Zn^{2+},Y^{3+}, Nd^{3+}) at the rutile-water interface. Santos et al.[42] studied the electrical double layer (EDL) formed by Na^+, K^+, and Cl^- ions near the walls of calcite mesopores. They found that the cation type and cation concentration affect their mobility and adsorption on the surface, which has an impact on the water structure. Koleini et al.[43] conducted molecular dynamics simulations for the calcite/brine interface in the presence of Na^+, Mg^{2+}, Cl^-, and SO_4^{2-}. They found that monovalent Na^+ and Cl^- ions form an EDL at the interface, while divalent ions do not. However, they did not discuss in detail the effect of specific ion concentration on the properties of interfacial water on calcite.

In a prior work from our group, Le et al.[29] studied the wetting properties of water on calcite as a function of CO_2 pressure. Two force fields were implemented to describe the water-calcite interactions, and the simulations predicted rather different contact angles. To complement that study, as well as to further investigate the properties of aqueous salt solutions at contact with mineral surfaces, we analyse here the effects of varying concentrations of NaCl, KCl, and $MgCl_2$ on the structure and dynamics of interfacial water on calcite. We compare the results obtained when the force fields developed by Xiao et al.[44] and Raiteri et al.[45] are implemented to describe water-calcite interactions. The calcite force field from Raiteri et al.[45] employs Buckingham-type potentials for carbonate - water interactions. In order to enable the use of

standard mixing rules when it is desired to describe in simulations the interactions of calcite with other species, Shen et al.[46] fitted the Buckingham potentials to Lennard-Jones functional forms by reproducing the hydration energies of calcium and carbonate ions, allowing us to perform simulations with salts dissolved in water.

The remainder of the manuscript is organized as follows: In Section 2, we describe the force fields and simulation setup and algorithms. In Section 3, we provide detailed analysis of the effects of Na^+, K^+, and Mg^{2+} ions on the relevant properties of water. We also compare the results obtained from the use of the two force fields mentioned above, specifically on the predicted properties of interfacial water. Finally, a summary of our main observations is provided in Section 4.

2. SIMULATION METHODS AND ALGORITHMS

Force Fields. The calcite surface was obtained from a calcite crystal terminated at the $10\bar{1}4$ plane.[25] In this model, calcium and carbon atoms were kept rigid, while the oxygen atoms were allowed to move. The rigid simple point charge extended (SPC/E)[47] and Joung-Cheatham (JC)[48] force fields were used to describe water and monovalent (NaCl and KCl) ions, respectively. Electronic Continuum Correction (ECC) forcefields developed for magnesium[49] and chloride[50] ions were applied to describe $MgCl_2$. These force fields were developed consistently with the SPC/E model of water. Standard force fields using full charges to describe divalent ions do not capture accurately ion pairing in aqueous solutions and overestimates the strength of ion-ion interactions with respect to ion-water interactions.[51,52] ECC forcefields scale the charges of all multivalent ions by the inverse square root of the electronic part of water dielectric constant and reduce the radius of each ion to achieve the required ion-water distances.[49,53] This method improves the description of the structure of the multivalent ions in electrolyte solutions significantly compared to standard approaches.[49-51] In the development of the force field by Xiao et al.,[44] the transferable intermolecular potential three-point model (TIP3P)[54] was used to treat water. TIP3P is part of the CHARMM simulation package and it is often used in simulations of biological systems.[55] In our prior investigation, we found that the structure of SPC/E water on the model of calcite described by the Xiao et al.[44] is very similar to that obtained when the TIP3P water model is used.[29] Further, when combined with SPC/E water, the JC force field gives reasonable results for the solubility of NaCl in water at ambient temperature, compared to experimental values.[56] Therefore, the SPC/E water model was chosen here.

In our simulations, dispersive forces were modelled by the 12–6 Lennard-Jones (LJ) potential and electrostatic forces were considered for non-bonded interactions. The cut-off distance for all interatomic interactions was set at 12 Å. The particle mesh Ewald (PME)[57] method was applied for long-range electrostatic interactions. The Lorentz-Berthelot mixing rule[58] was applied for the calculation of the LJ parameters for unlike atoms.

Simulation Setup. An illustration of the simulation box is presented in Figure 1. The simulation box was periodic in the three directions and it contained a thin film of fluid on a slab of calcite. The initial configuration consists of 14,000 water molecules placed on the calcite surface. The x, y and z dimensions of the simulation box were 97.14, 90.0, and 158.9 Å, respectively. In the simulations, the calcite substrate, with a thickness of 14.1 Å, was placed parallel to the x-y plane. The number of salt ions inserted was adjusted to vary the concentration between 1 – 3 M. These concentrations are below the solubility limit for the various simulated electrolytes at ambient conditions.[49,56,59-61] The thickness of the aqueous film on calcite was 45 – 50 Å, depending on composition. The remaining space in the z direction, above the film, was left empty. The dimensions of the box and the relatively large amount of water included in the simulations were chosen to ensure that the periodic boundary conditions did not affect the results, and to allow for establishing 'bulk-like' water in the middle of the thin film, whose properties differ from those of the two interfacial regions (solid-liquid and liquid-gas), respectively.

Algorithms. The simulations were carried out with the packages GROMACS (version 5.1.4)[62,63] and LAMMPS (version 20180818),[64] using the canonical NVT ensemble, where the number of particles (N), the simulation volume (V), and the temperature (T) are kept constant. We implemented the Nosé-Hoover thermostat[65,66] with a relaxation time of 100 fs to maintain the temperature at 298 K. The SETTLE algorithm[67] was used to keep bonds and angles within the water molecules fixed. The total simulation time was 60 ns. The system was considered equilibrated when the atomic densities stabilized and both energy and temperature of the system remained within 10% of their average values. The last 2 ns of the simulations were used for production. Each simulation was repeated twice to increase reliability.

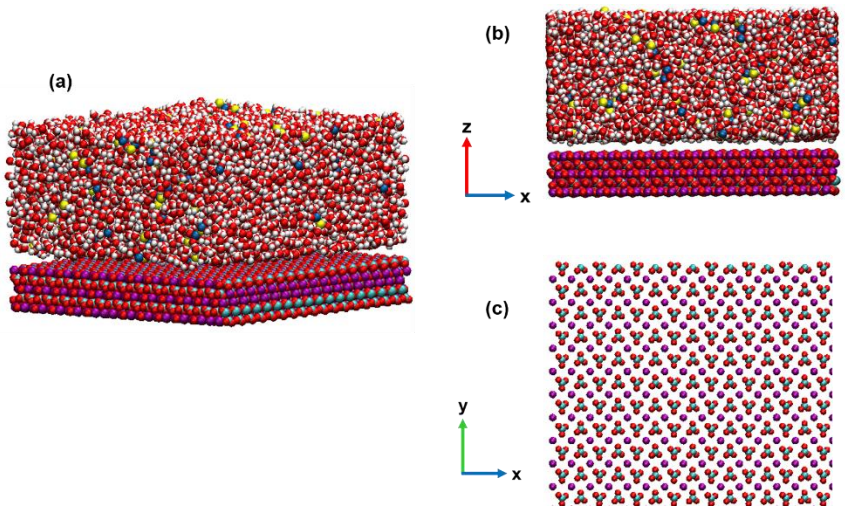

Figure 1. Representative simulation snapshots of the initial configuration of the system (a) and (b) and top view of the calcite substrate surface (c). Ca = purple; C = cyan; O = red; H = white; Na, K, Mg = yellow; Cl = blue.

3. RESULTS AND DISCUSSION

3.1. Atomic Density Profiles

The atomic density distributions of oxygen and hydrogen atoms of water molecules, as well as those of cations (Na^+, K^+, and Mg^{2+}) and Cl^- at different salt concentrations were calculated as a function of the perpendicular distance (z) from the calcite surface. The top plane of calcium atoms was used as the reference point (z = 0). The results shown in Figure S1 of the Supporting Information indicate that the density profiles in the z direction do not depend significantly on the cation and salt concentration, thus only the atomic density profiles obtained at 2 M salts concentration are presented in the main manuscript for brevity. In Figure 2, we provide the atomic density distribution of water oxygen (solid red line) and water hydrogen (broken brown line), monovalent (Na^+ and K^+) cations (solid blue line) and Cl^- ions (solid green line) for systems with 2 M NaCl and 2 M KCl.

The density profile for oxygen atoms shows the formation of four hydration layers near the surface, with two distinct layers at distances 2.5 and 3.5 Å, respectively. The first hydration layer is approximately twice the density of the second one, indicating that a large number of water molecules accumulate near the surface. The results are in agreement with previous molecular dynamics studies of interfacial water on calcite,[27] as well as with experimental X-ray reflectivity data.[28] The first three peaks in the hydrogen atomic density profile appear at 2.5, 3.1 and 3.9 Å, respectively. Comparing the intensities and widths of hydrogen and oxygen density peaks suggests that most water molecules in the first hydration layer maintain one of the OH bonds either parallel to or pointing away from the surface. The second water oxygen peak at 3.5 Å is accompanied by water hydrogen peaks at 3.1 and 3.9 Å. This suggests some of the water molecules in the second hydration layer have some of their OH bonds pointing towards the calcite surface, while others point away from it. We will subsequently analyse the orientation of interfacial water in more detail.

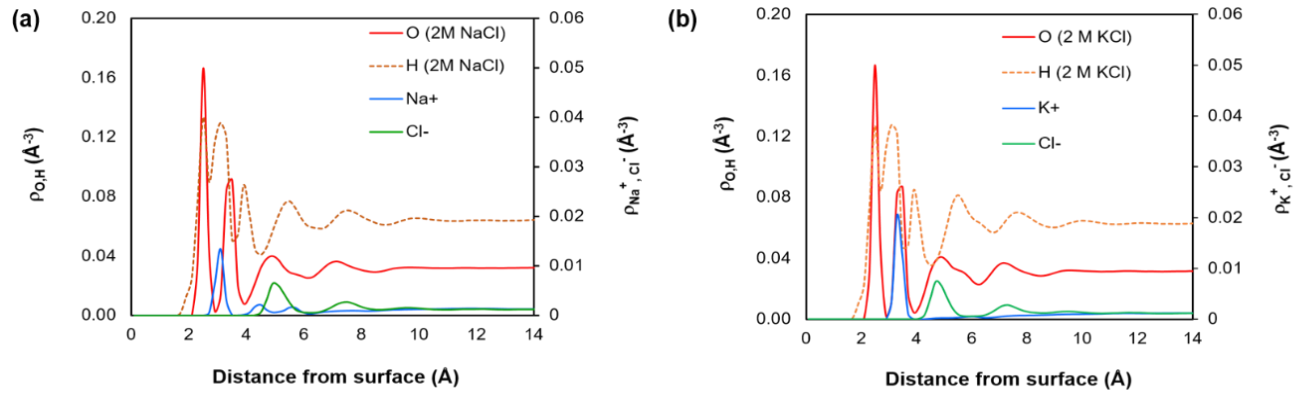

Figure 2. Atomic density profiles along the z direction, vertical from the surface, for (a) water and salt ions at 2 M NaCl (b) water and salt ions at 2 M KCl. The reference (i.e., z = 0) is defined by the z-position of the plane of the top calcium atoms on the calcite surface. These simulations were conducted using the force field proposed by Xiao et al.[44] to describe calcite and they were conducted at 298 K.

The Na^+ density profile (Figure 2a) shows a pronounced peak at 3.1 Å in between the first and second hydration layers. This peak is closer to the second hydration layer than the first, suggesting stronger interactions between the Na^+ ions and the water molecules in the second layer than with water in the first hydration layer. This could also be due to the strong interactions between calcite and water molecules in the first hydration layer, making it more difficult for salts to penetrate the first hydration layer. By comparison, the K^+ ion profile (Figure 2b) is characterized by a peak at 3.3 Å. Due to their larger ionic radius, K^+ ions adsorb 0.2 Å further from the surface compared to Na^+. The Na^+ and K^+ peaks are close to the surface, as observed in Figures 2a and 2b, whereas the Cl^- peaks are less dense and are found further from the surface at 5.1 Å. These results, as highlighted from simulation snapshots in Figure 3a and 3b, suggest that the ions form an EDL on the surface, with Na^+ and K^+ ions in the Stern layer and Cl^- ions in the diffuse layer. It is worth noting that in all the density profiles, as the distance from the surface becomes greater than 10 Å, we observe smooth bulk water/salt density profiles, reflecting the uniform salt concentration expected in bulk water.

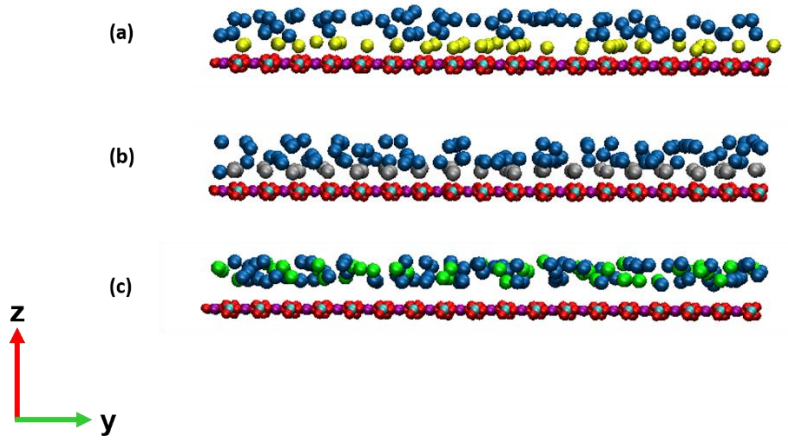

Figure 3. Simulation snapshots illustrating the electrical double layer (EDL) formed by aqueous NaCl (a), KCl (b) and $MgCl_2$ (c) ions on calcite. Ca = purple; C = cyan; O = red; Na =yellow; K=grey; Mg=green; Cl = blue. Water molecules are present but are not shown for visualisation purposes. The simulations were conducted using the force field proposed by Xiao et al.[44]

In Figure 4, we report the density profiles in the system with 2 M $MgCl_2$ and find that despite being the smaller ion in the study, the profile for Mg^{2+} is characterized by a wider peak ~ 5.3 Å from the surface, where it is almost fully hydrated, due to its high charge density. This means most of the Mg^{2+} ions maintain their strong hydration shells and remain further from the surface, as a result of strong interactions with water. In addition, both the density profiles in Figure 4 and the simulation snapshot in Figure 3c show Mg^{2+} and Cl^- ions occupy the same layer. The results indicate that monovalent ions have stronger interactions with calcite, as suggested by the formation of inner-sphere complexes of Na^+ and K^+ ions at the calcite-water interface while Mg^{2+} ions adsorb as outer-sphere complexes. These results highlight the

importance of a balance between ion hydration and ion-surface interactions in determining the salt ions distribution near the calcite-water interface.

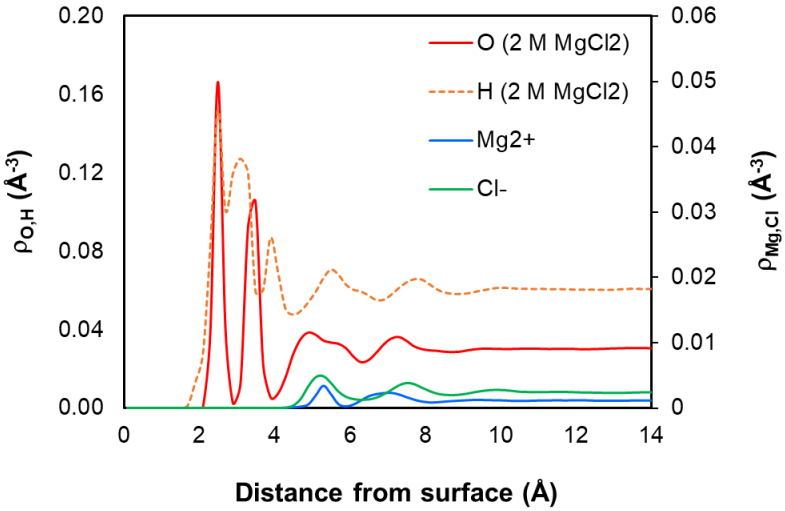

Figure 4. Atomic density profiles along the z direction, vertical from the surface, for water and salt ions at 2 M $MgCl_2$. The reference (i.e., z = 0) is defined by the z-position of the plane of the top calcium atoms on the calcite surface. These simulations were conducted using the force field proposed by Xiao et al.[44] to describe calcite and they were conducted at 298 K.

The results discussed so far were obtained using the force field proposed by Xiao et al.[44] to describe calcite. Figure 5 provides a comparison of the oxygen and hydrogen density profiles obtained when the force field developed by Raiteri et al.[45] is implemented instead. We observe a slight difference in the predicted structure of water. The first two hydration layers in the system simulated using the Buckingham potentials proposed by Raiteri et al.[45] to describe calcite are less dense and found at ~ 2.15 and 3.25 Å, respectively, from the calcite substrate whereas the peaks in the density profile for hydrogen atoms are at ~ 2.35 and 3.05 Å, respectively. When the fitted LJ parameters developed by Shen et al.[46] are applied instead of the Buckingham potential, the peaks of the first and second hydration layers are located at 2.15 and 3.45 Å, respectively, and their intensity changes somewhat as well, suggesting that the LJ parameterisation does not fully reproduce the properties of interfacial water on calcite as described by the potential proposed by Raiteri et al.[45] There is also a difference in the directions of the OH bonds depending on the force field implemented. Specifically, when the force field of Raiteri et al.[45] and Shen et al.[46] are implemented, the results suggest the water molecules in the first hydration layer point their OH bonds away from the calcite substrate. In contrast, they predict some of the water molecules in the second hydration layer adopt a hydrogen-down orientation, while the others project their hydrogen atoms away from the surface. The experimental X-ray reflectivity data[24,28] only provide the position of the hydration layers, as identified by the position of the absorbed layer of the oxygen atoms of water on calcite. Within the uncertainty of both experiments and simulations, the experimental data do not allow us to discriminate whether the force field of Xiao et al.,[44] or that of Raiteri et al.,[45] is more reliable for predicting the structure of interfacial water. In comparing the Na^+ density profile from both

force fields (Figure S2), we observed that the force field of Raiteri et al.[45] leads to a peak ~ 0.2 Å closer to the surface and approximately five times denser than that proposed by Xiao et al.[44] This could be due to a strong difference in terms of electric double layer forces exerted by calcite wetted by concentrated brines.

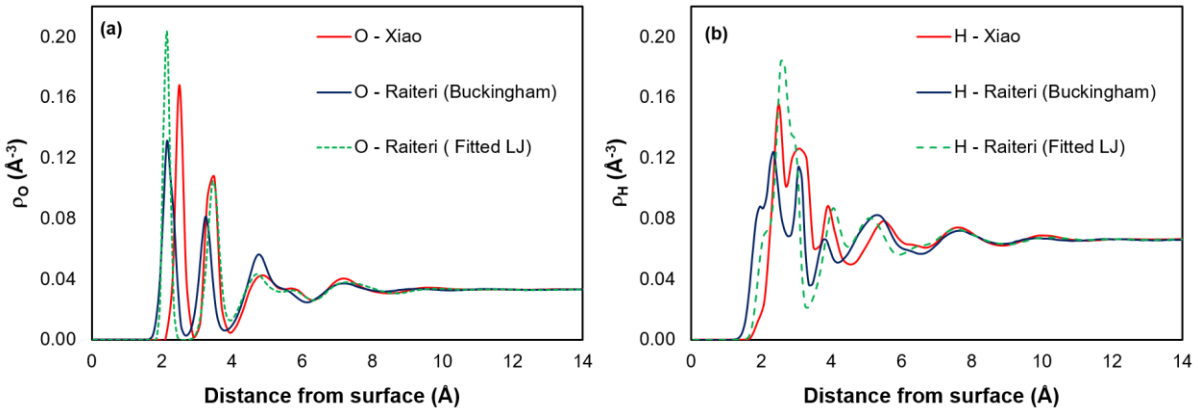

Figure 5. Atomic density profiles along the z direction, vertical from the surface, for oxygen atoms (a) and hydrogen atoms (b) of water molecules in systems with no salt. These results were obtained from simulations in which calcite is described by the force field developed by Xiao et al.[44] or Raiteri et al.[45] The top plane of calcium atoms on the calcite surface was used as the reference (z = 0). The simulations were conducted at 298 K.

3.2. Planar Density Distributions

To relate the structure of interfacial water to the properties of the solid substrate, we computed the surface density distributions of water oxygen and hydrogen atoms within the first two hydration layers within the x-y plane parallel to the surface, at different salt concentrations. In the simulations conducted with the force field of Xiao et al.,[44] the positions of the hydration layers are identified from the peaks in the atomic density profiles of oxygen atoms in Figure 2 and Figure 4. The first hydration layer is located at ~ 2.9 Å from the surface; the second hydration layer is located at ~ 3.9 Å. For the purpose of clarity, only results for systems with no salts and 2 M salt concentrations are shown. The results presented in Figure 6 show the preferential distribution of oxygen atoms, with well-defined areas of very high densities, in the first and second hydration layers. The oxygen atoms in the first hydration layer manifest a somewhat more organized structure than those in the second hydration layer, evident from the slightly more concentrated areas of high water densities. This could be attributed to the stronger interactions of water molecules with the calcite substrate. Adding NaCl and KCl ions leads to a distortion in the arrangement of water molecules in the hydration layers. As highlighted by the circles in panels (f) and (g), the effect is somewhat more pronounced in the second layer than in the first, confirming stronger interactions between Na^+ and K^+ ions with water molecules in that layer, as suggested by the atomic density profiles (Figure 2). The presence of divalent Mg^{2+} ions produces no significant difference in the surface distribution of water oxygen, consistent with the density profiles shown in Figure 4, which suggests Mg^{2+} ions accumulate further from the surface compared to Na^+ and K^+ ions.

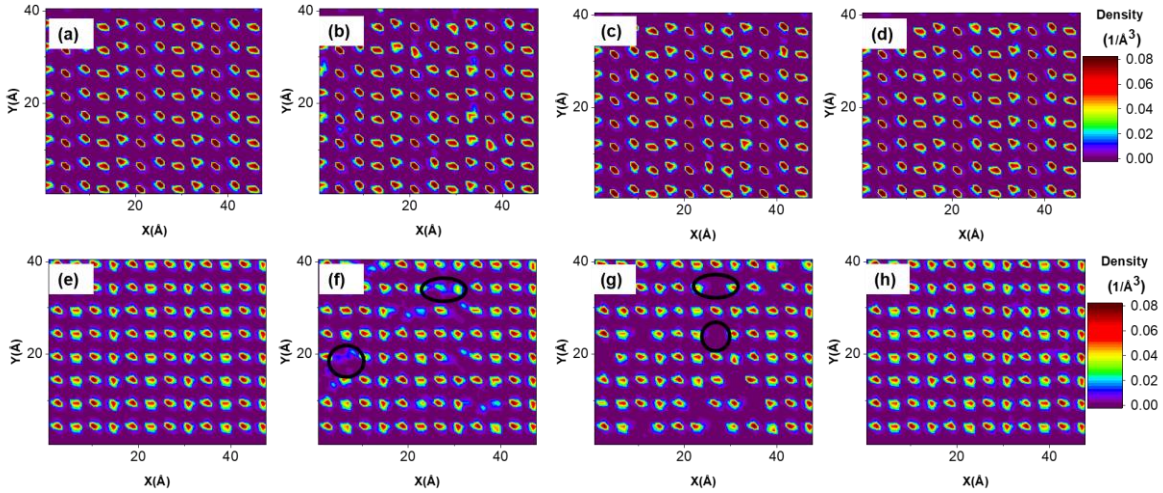

Figure 6. Surface density distributions of water oxygen atoms in the first (panels (a) - (d)) and second (panels (e) - (h)) hydration layers on calcite for systems with no salts (panels (a) and (e)), 2 M NaCl (panels (b) and (f)), 2 M KCl (panels (c) and (g)) and 2 M $MgCl_2$ (panels (d) and (h)). The simulations were conducted using the force field of Xiao et al.[44] to describe calcite. The colour bar expresses density in the units of 1/Å^3. The black circles highlight regions where the water structure is affected by the salt ions (see text for details).

In Figure 7, the positions of the atoms on the top plane of the surface are compared with the planar density distributions of oxygen atoms for systems with no salts, in the first and second hydration layers (panels (a) and (b), respectively). The results suggest the calcium atoms on the substrate provide adsorption sites for water molecules in the first hydration layer, which is consistent with the observations reported by Zhu et al.[27] in their study of aqueous biomolecules near calcite. In the second layer, however, oxygen atoms seem to accumulate in regions corresponding to the planar location of the carbon atoms of the carbonate ions in calcite. In panel (c) of Figure 7, we highlight the configuration of water molecules in the second hydration layer interacting with the surface C atoms.

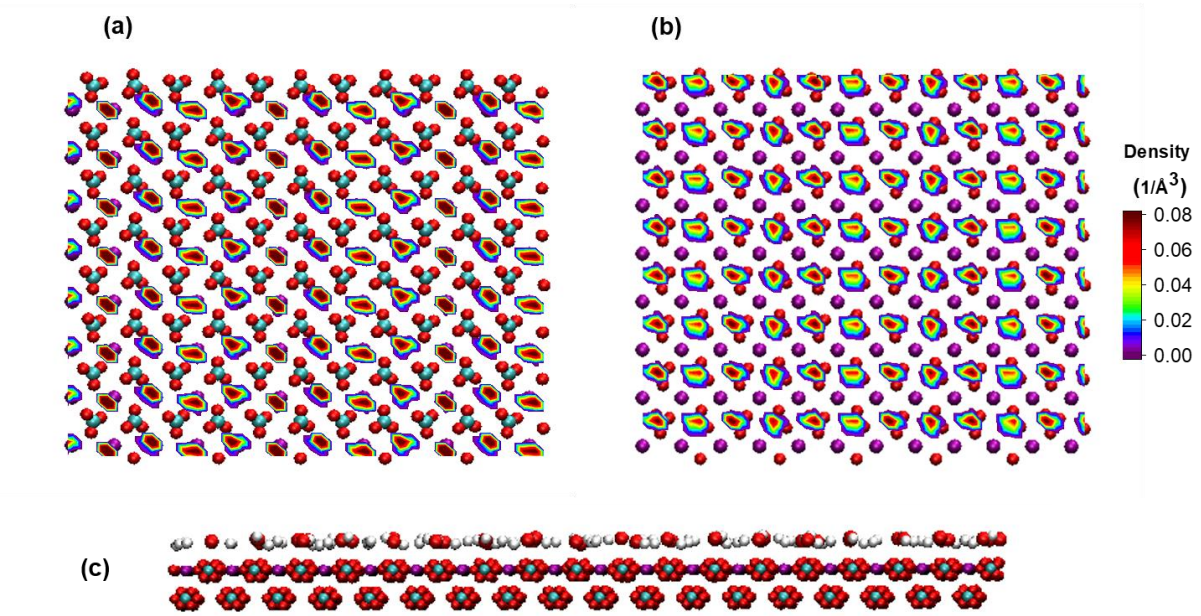

Figure 7. Simulation snapshots of the adsorption of oxygen atoms of water in the first (a) and second (b) hydration layers on the calcium atoms of calcite and interactions between water in the second hydration layer and carbonate ions. Ca = purple; O = red; C = cyan; H = white. These simulations were conducted using the force field proposed by Xiao et al.[44]

The positions of the first and second layer of hydrogen atoms, as identified in Figure 2, are ~ 2.7 Å and 3.5 Å from the surface, respectively. Figure 8 shows that the arrangement of the hydrogen atoms is less organized compared with that of the oxygen atoms, with the hydrogen atoms in the second layer presenting a more uniform planar distribution than those in the first hydration layer. As the salinity increases, there is greater distortion of the planar distribution, as highlighted by areas with little to no hydrogen atoms. KCl clearly causes greater disruption in the arrangement of water molecules than NaCl, as observed by the increased number of areas with no oxygen and hydrogen atoms, which is consistent with the observations reported by Marcus[68], according to whom K is more of a 'structure breaker' than Na. In the presence of Mg^{2+}, we observe little difference in the surface distribution of water oxygen and hydrogen atoms compared to when no ions are present in the system, in agreement with the vertical density profiles shown in Figure 4.

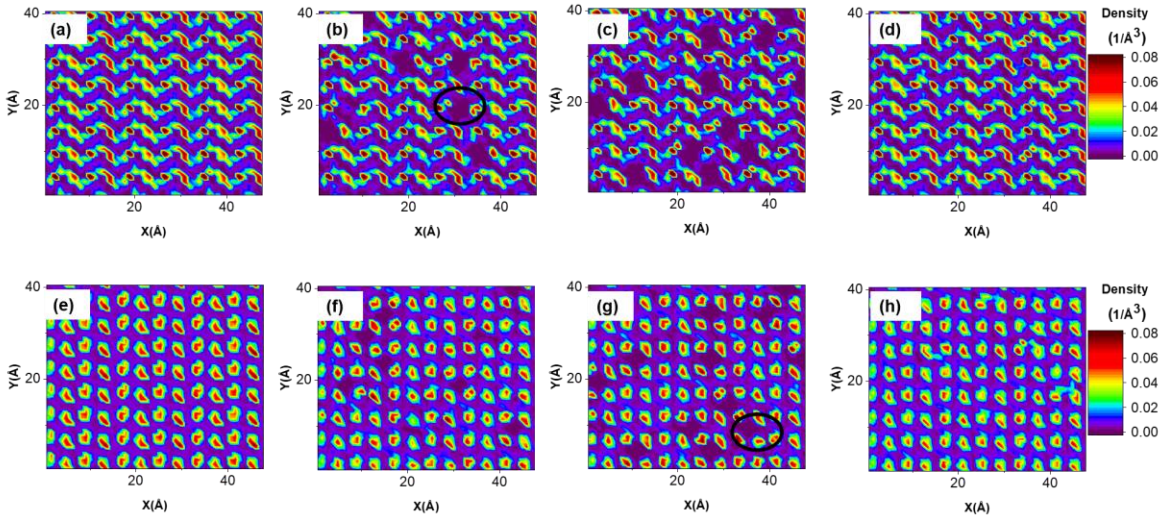

Figure 8. Surface density distributions of water hydrogen atoms in the first (panels (a) - (d)) and second (panels (e) - (h)) hydration layers on calcite for systems with no salts (panels (a) and (e)), 2 M NaCl (panels (b) and (f)), 2 M KCl (panels (c) and (g)) and 2 M $MgCl_2$ (panels (d) and (h)). The simulations were conducted using the force field proposed by Xiao et al.[44] to describe calcite. The colour bar expresses density in the units of 1/Å^3.

To quantify the disparity between the planar density distributions predicted by the two force fields applied to model calcite, we calculated the difference between the results for each force field. It should be noted that the Raiteri et al.[45] force field yields first and second hydration layers at ~ 2.65 Å and 3.85 Å, respectively whereas the first of two layers from the hydrogen atom density profile is located at ~ 2.75 Å and 3.35 Å from the surface. In the results shown in Figure 9, positive values correspond to the positions where the force field proposed by Xiao et al.[44] predicts higher densities than that of Raiteri et al.,[45] while the opposite holds for negative values. In general, the force field of Raiteri et al.[45] leads to different structure of water on the first and second layers, although it should be recognised that the planar distributions of Figure 9 show that, in most of the interfacial area, the atomic densities predicted by the two force fields are very similar.

To complement these planar density profiles results, In Figure S3, we present the surface density distributions of oxygen and hydrogen atoms in the second hydration layer for pure water and 2 M NaCl systems when calcite is represented by the Raiteri et al.[45] force field. We focus on the second hydration layer because our simulation results suggest that the ions accumulate in its proximity. The results suggest that the presence of 2 M NaCl ions has a more profound effect on interfacial water when the force field proposed by Raiteri et al.[45] is implemented, as observed from the difference compared to the results obtained in Figure 6 (panel f), when the Xiao et al.[44] force field is used. This is probably because the Raiteri et al.[45] force field predicts a substantially larger accumulation of Na^+ ions near calcite compared to the Xiao et al.[44] force field (see Figure S2).

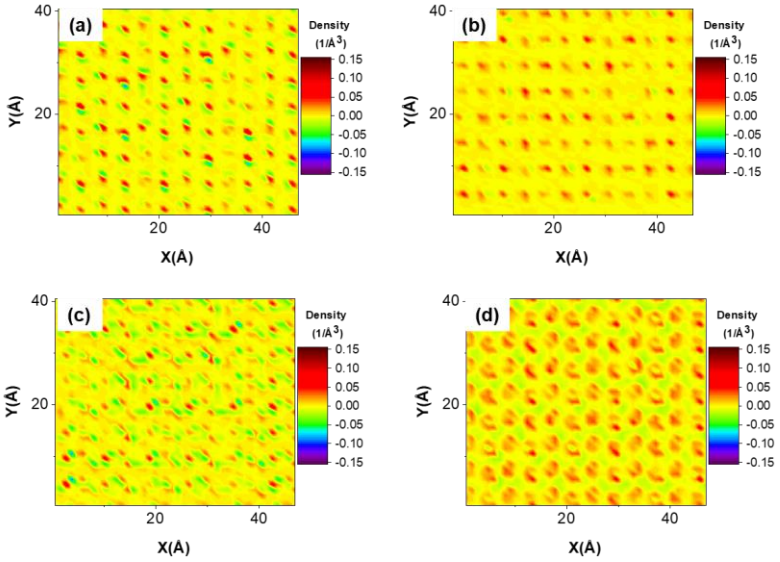

Figure 9. Difference in surface density distributions from simulations carried out implementing the force fields by Xiao et al.[44] and Raiteri et al.[45] to describe the water-calcite interactions. The results are shown for water oxygen (panels (a) and (b)) and hydrogen (panels (c) and (d)) atoms in the first (panels (a) and (c)) and second (panels (b) and (d)) hydration layers. The colour bar expresses density in the units of 1/Å^3.

3.3. Radial Distribution Functions

The radial distribution function (RDF) is used to quantify the structure of interfacial water based on the Xiao et al. force field. In Figure 10**,** we report the in-plane oxygen-oxygen and hydrogen-hydrogen RDFs within the first two hydration layers. The results are compared to those obtained for water molecules found at distances greater than 13 Å from the top plane of calcium atoms on the surface, which were considered representative of bulk water for the present study. The latter results are found to be similar to those reported from previous studies at ambient conditions.[69-72]

The RDFs results within the first two hydration layers are consistent with ordered structure, which is attributed to the interactions between water molecules in these layers and calcite. There is a small peak on oxygen – oxygen RDF for water in the second hydration layer at radial distance ~ 2.8 Å, which is in the same position as the first peak observed for bulk water. In contrast, the first peak observed in the first hydration layer is close to 5 Å, suggesting water molecules in this layer are not close enough to form hydrogen bonds. The distance between the peaks observed in the RDFs corresponds approximately to the distance between the high-density areas observed in the planar density distribution of oxygen atoms shown in Figure 6. Although calcite clearly perturbs the water structure in the first two hydration layers, our results (Figure S4) suggest that the radial density distributions do not depend strongly on the force field implemented to describe the solid substrate, nor on the cation types or on the overall salt

concentration. The latter is because none of the ions simulated strongly perturbs the hydration layers, with Na^+ and K^+ only distorting, to a small extent, the second hydration layer.

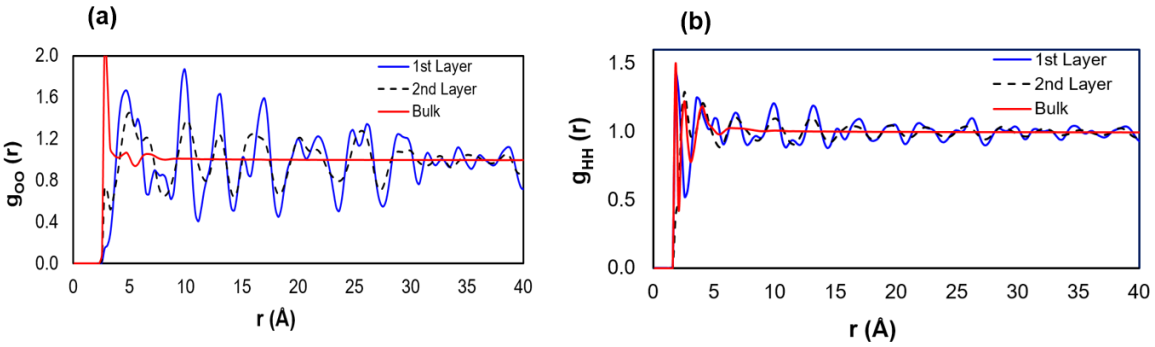

Figure 10. Oxygen-Oxygen (a) and Hydrogen-Hydrogen (b) radial distribution functions for water molecules in the first and second hydration layers, as well as in the bulk (>13 Å) for systems with 2 M NaCl. These simulations were conducted using the force field proposed by Xiao et al.[44] to describe calcite. The simulated temperature was 298 K. Similar results were obtained when the Raiteri et al.[45] force field was used to describe water-calcite interactions.

In Figure 11, we report RDFs for ions – oxygen atoms of water (OW) in the first and second hydration layers, as well as in the bulk. The results clearly show that the interactions between water and Na^+ ions in the second hydration layer are bulk - like.[73,74] Conversely, the RDF is highly distorted for the first hydration layer, presumably because the proximity to the calcite substrate affects the structure of water as well as its ability to interact with other species. The interactions of Na^+ and oxygen atoms in the second hydration layer are bulk-like, whereas the RDFs between K^+ or Mg^{2+} and water in the second hydration layer are similar to those obtained for the first hydration layer. The positions of the peaks in the RDF involving bulk water and KCl agree with previous observations.[73,75-77] The Mg-OW(bulk) RDF is also in agreement with previous studies.[78,79] The solvation shell of Mg^{2+} is the tightest, as shown by the sharp peak at ~ 2.06 Å, because of the three cations considered, it has the smallest ionic radius. The peaks of Na-OW and K-OW are at found at 2.31 Å and 2.81 Å, respectively. As the ionic radius of the cation increases, the peaks in the RDF are found at larger distances and are smaller and wider, suggesting that smaller ions are bound more strongly to water molecules than larger ions. In Figure S5, we observe a slight difference in the radial distribution functions obtained from the implementation of the two force fields to describe water-calcite interactions.

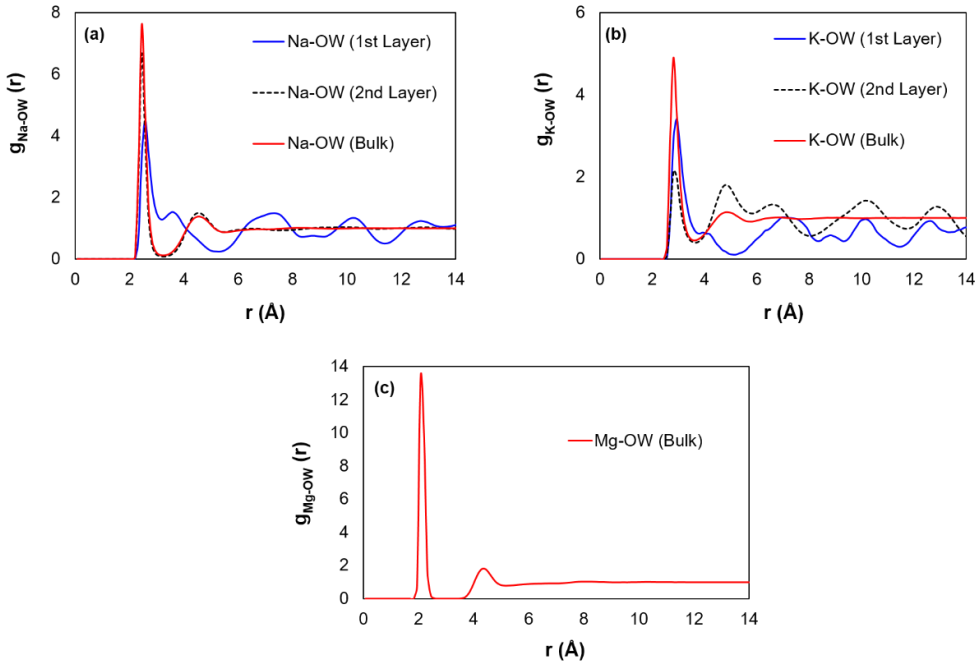

Figure 11. Radial distribution functions between water oxygen atoms and Na^+ (a), K^+ (b), and Mg^{2+} (c) ions in the first and second hydration layers and bulk (>13 Å) for systems with 2 M salts. These simulations were conducted using the force field proposed by Xiao et al.[44] to describe calcite and they were conducted at 298 K.

From the RDFs, we calculated the coordination number of Na^+ ions in the first two hydration layers, as well as in the bulk, by integrating the first peak on the relevant RDFs:[73]

$$n_c = 4\pi\rho \int_0^R r^2 g(r) dr \qquad (1)$$

In Eq. 1, ρ is the average density, r is the radial distance, and R is the upper limit of the radial distance in the first peak of the RDF. In Table 1, we present the coordination number of one Na^+ ion in the first and second hydration layers and in bulk water, which is consistent with literature data.[73,74] The coordination number of Na^+ reduces slightly as the NaCl concentration increases. The higher hydration number in the first layer could be due to the increased number of water molecules in this layer and the lower number of Na^+ ions, when compared to the second hydration layer.

Table 1. Coordination number of Na^+ in the first solvation shell of water in the first and second hydration layers and bulk (>13 Å) for systems with 1 – 3 M NaCl, conducted using the force field proposed by Xiao et al.[44] to describe calcite.

	1st Layer	2nd Layer	Bulk
1 M	6.6	4.7	5.9
2 M	6.5	4.7	5.7
3 M	6.2	4.7	5.6

The results provided in Table 2 show that K^+ ions have the largest hydration number while Mg^{2+} has the smallest, which is consistent with other simulations.[73,74,78] The force field by Raiteri et al.[45] yields smaller hydration shells around Na^+ compared to the outcome determined from Xiao et al.[44] This could be due to the very dense layer of Na^+ observed in Figure S2.

Table 2. Coordination number of cations in the first solvation shell of water in the first and second hydration layers and bulk (>13 Å) at 2 M. These simulations were conducted using the force field proposed by Xiao et al.[44] and Raiteri et al.[45] to describe calcite.

	1st Layer	**2nd Layer**	**Bulk**
Na^+	6.5	4.7	5.7
K^+	6.7	3.9	6.9
Mg^{2+}	-	-	5.6
Na^+ (Raiteri LJ)	4.2	2.9	5.7

3.4. Molecular Orientation

The orientation of interfacial water molecules was quantified based on the angle (θ) between the water dipole moment and the vector perpendicular to the surface. Angles of 0° and 180° correspond to OH bonds pointing away from, and towards the surface, respectively. When the angle is 90°, one of the OH bonds in a water molecule is projected away from the surface while the other is projected towards the surface. Figures 12 and 13 present the probability distributions P[cos(θ)] for water molecules in the first and second hydration layers, which are compared to the results obtained for bulk water. Although the effects of ions were observed at 1 – 3 M salts, only results for systems with no salts and 2 M salts are presented.

The results for bulk water show a uniform distribution of orientation, while water molecules in the first two hydration layers show pronounced preferential orientations. When no salt is present, the results obtained from the two force fields implemented for the solid substrate are similar, although some differences are evident. When the force field by Xiao et al.[44] is used, a pronounced peak near cos(θ) ~ 1, suggests the water molecules in the first hydration layer have a strong preference to form 10° angles between their dipoles and the vector normal to the surface, corresponding to OH bonds pointing away from the surface. In this layer, oxygen atoms interact with calcium ions of calcite while hydrogen atoms from hydrogen bonds with oxygen atoms in the second hydration layer. The force field by Raiteri et al.[45] and Shen et al.[46] also predict higher percentage of water in the first hydration layer having their dipoles ~ 45 – 90° to the surface normal. These results differ from those obtained for water at the interface with other substrates. For example, Argyris et al.[17] predicted that water molecules near silica surface point some of their OH bonds towards the surface. The addition of NaCl and KCl (Figure 13) increases the probability of finding water dipoles at ~ 10° to the vector normal to the surface and causes a reduction in the probability of water molecules maintaining their dipoles at angles ~ 47° – 90° to the vector normal to the surface.

In contrast, for both force fields, the probability distribution for the orientation of water in the second hydration layer is characterized by a wider peak at angles corresponding to ~ 110° – 120°. At least one OH bond of water in this layer points slightly towards the surface to form hydrogen bonds with water in the first hydration layer and to interact with the carbonate ions of calcite. For the force field proposed by Xiao et al.,[44] the addition of NaCl and KCl ions leads to a shift in the preferential orientation of water to a slightly smaller angle. The implementation of the LJ parameters proposed by Shen et al.[46] yields more water molecules having their OH bonds pointing away from the surface as 2 M NaCl is added to the system. The difference in the molecular orientation within the two hydration layers suggests calcite strongly restricts the orientation of interfacial water especially within the first hydration layer.

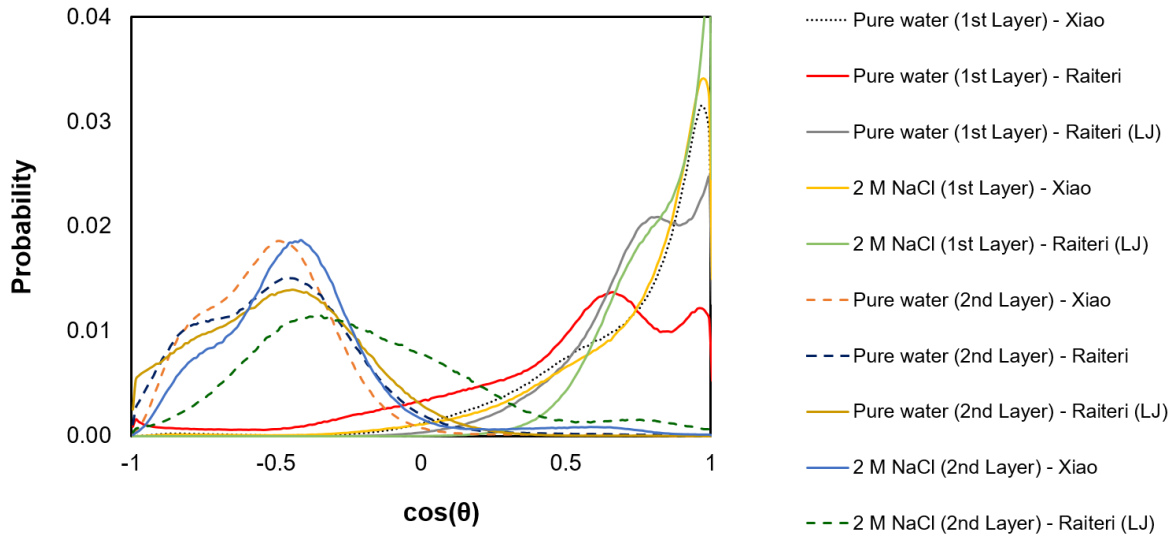

Figure 12. Orientation of water molecules displayed as probability distribution of the cosine of the angle for systems with no salts and 2 M NaCl simulated by implementing the force field developed by Xiao et al.[44], Raiteri et al.[45] and Shen et al.[46] to model calcite. The simulated temperature was 298 K.

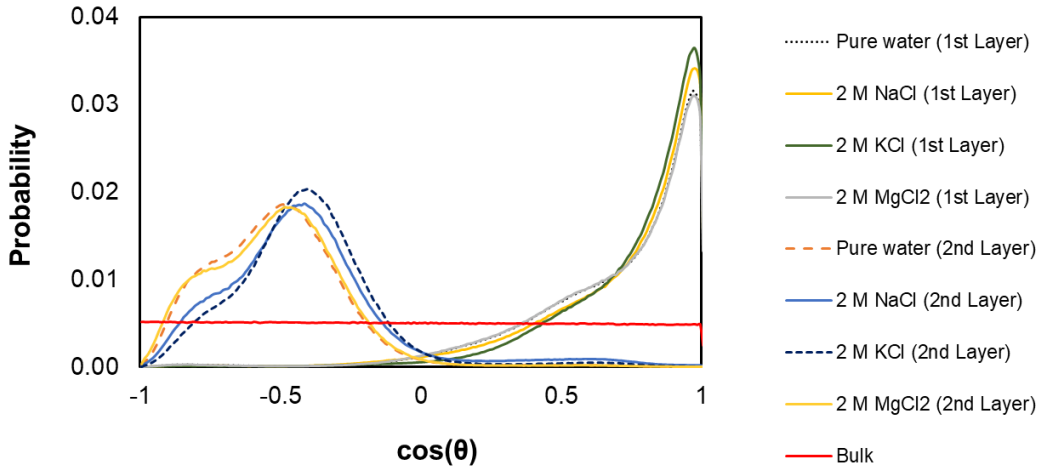

Figure 13. Orientation of water molecules displayed as probability distribution of the cosine of the angle for systems with no salts and 2 M NaCl, 2 M KCl and 2 M $MgCl_2$, simulated with the force field developed by Xiao et al.[44] to model calcite. The simulated temperature was 298 K.

3.5. Hydrogen Bond Network

To further evaluate the effects of salts on the structure of interfacial water, we computed the hydrogen bond density profiles for water molecules as a function of the distance (z) perpendicular to the calcite surface, at various salt concentrations. Following the geometric criterion defined by Marti,[80] water molecules were considered hydrogen bonded if the distance between an hydrogen atom in one water molecule and the oxygen atom in another water molecule was less than 2.4 Å, and the correspondent H−O···O angle was less than 30°. To calculate the hydrogen bond density profiles (Figure 14), the position of a hydrogen bond was taken as mid-distance between the positions of the oxygen and hydrogen atoms in the hydrogen bond.

There are three pronounced peaks evident in Figure 14a, with a reduction in the hydrogen bond densities as the concentration of NaCl increases. The density profiles discussed above (e.g., Figure 5) suggest that interfacial water yields four hydration layers, with the first two being well pronounced, and the latter two being less evident. The hydrogen bond density profiles (Figure 14a) seem to confirm the presence of four hydration layers. In fact, the first peak at 3.1 Å suggests hydrogen bonds formed between water molecules in the first and second hydration layers or between water molecules within the second hydration layer. The second peak in the hydrogen bond density profiles, found at 3.9 Å, is likely representative of hydrogen bonds between water molecules in the second and third hydration layers. The less intense peak at ~ 6.3 Å indicates hydrogen bonds between the third and fourth hydration layers. Being third and fourth hydration layers not well pronounced, also the peak in the hydrogen bond density profile is less intense than those closer to the surface. At distances greater than ~ 10 Å, the hydrogen bond density distribution becomes uniform, representative of bulk water.

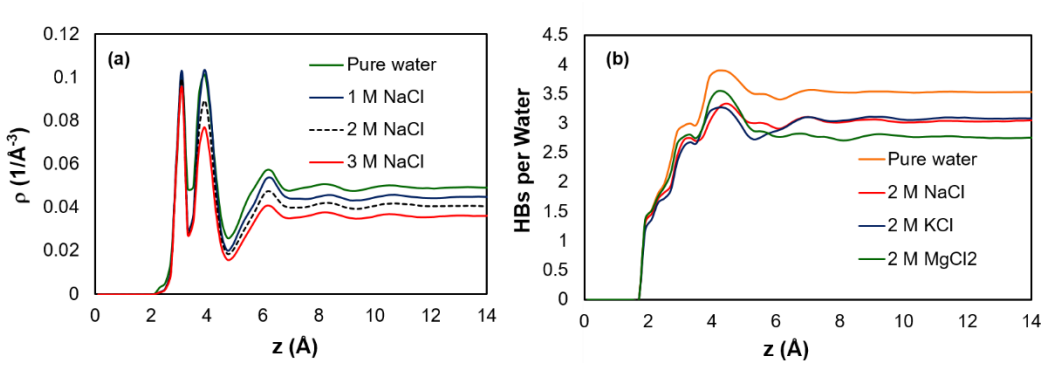

Figure 14. Density profiles of water−water hydrogen bonds along the distance perpendicular to the surface for systems with pure water and 1-3 M NaCl (a) and (b) number of hydrogen bonds per water molecule as a function of perpendicular distance from the surface for systems with pure water, 2 M NaCl, 2 M KCl and 2 M $MgCl_2$. The reference (i.e., z = 0) is defined by the z-position of the plane of calcium atoms on the calcite surface. These simulations were conducted using the force field proposed by Xiao et al.[44] to describe calcite and at 298 K.

To compare the effects of cations and the force field implemented to describe calcite on the hydrogen bond network, we calculated the number of hydrogen bonds (HBs) per water molecule, as a function of distance (z) perpendicular to the calcite surface. The results in Figure 14b, from the implementation of the force field of Xiao et al.,[44] show the number of hydrogen bonds per water molecule in the first and second hydration layers do not vary significantly with the type of cations in the system, in comparison to the bulk. In Table 3, we present the average number of hydrogen bonds per water molecules in the first two hydration layers and the bulk. While there is a reduction in the number of hydrogen bonds per water in the first and second hydration layers upon the addition of ions, Mg^{2+} ions reduce the number to a lesser extent due to most of the ions being found further from the surface, as observed in Figure 4. In bulk water, there are approximately 3.53 hydrogen bonds per water molecule in the pure water system, consistent with literature values.[81-83] This value reduces to ~ 3.04, 3.01 and 2.75 in systems with 2M K^+, Na^+ and Mg^{2+}, respectively. Although we observed similar trends in the hydrogen bonds from the force field of Raiteri et al.,[45] there are lower number of hydrogen bonds per water molecules in the first and second hydration layers, for pure water and 2 M NaCl systems, consistent with the force field proposed by Raiteri et al.[45] showing a dense layer of Na^+ ions closer to the surface.

Table 3. Number of hydrogen bonds per water molecule in the first and second hydration layers, and bulk, for systems with pure water, 2 M NaCl, 2 M KCl and 2 M $MgCl_2$. These simulations were conducted using the force field proposed by Xiao et al.[44] and Raiteri et al.[45] to describe calcite and at 298 K.

	Pure water	**2 M NaCl**	**2 M KCl**	**2 M $MgCl_2$**	**Pure water (Raiteri LJ)**	**2 M NaCl (Raiteri LJ)**
1st Layer	1.71	1.40	1.37	1.53	1.61	0.99
2nd Layer	3.01	2.64	2.57	2.78	2.83	2.39
Bulk	3.53	3.01	3.04	2.75	3.53	3.01

To achieve a better understanding of the interactions of water with the calcite surface, we quantified the formation of hydrogen bonds between hydrogen atoms in water and oxygen atoms in the carbonates of calcite. Following Wolthers et al.[82], we found (see Table 4), that most water molecules do not form hydrogen bonds with the carbonate surface considered here and that the number of hydrogen bonds is higher in the second hydration layer than the first, which is consistent with the orientation of water in these layers. The presence of ions reduces the number of hydrogen bonds formed, with KCl having the biggest impact in the first hydration layer while NaCl affects the hydrogen bonds in the second layer. In the implementation of the force field developed by Raiteri et al.,[45] carbonates form more hydrogen bonds with water in the first hydration layer but less with water in the second layer.

Table 4. Number of hydrogen bonds formed with oxygen atoms of surface carbonate groups, per water in the first and second hydration layers, for systems with pure water, 2 M NaCl, 2 M KCl and 2 M $MgCl_2$. These simulations were conducted using the force field proposed by Xiao et al.[44] and Raiteri et al.[45] to describe calcite and at 298 K.

	Pure water	**2 M NaCl**	**2 M KCl**	**2 M $MgCl_2$**	**Pure water (Raiteri LJ)**	**2 M NaCl (Raiteri LJ)**
1st Layer	0.15	0.14	0.13	0.15	0.20	0.16
2nd Layer	0.67	0.64	0.68	0.67	0.57	0.52

3.6. Residence Times

Residence autocorrelation functions $C_R(t)$ for water molecules have been used to describe the dynamical properties of interfacial water.[84,85] $C_R(t)$ quantifies the average time water molecules remain continuously within a particular hydration layer. $C_R(t)$ for a given molecule starts at 1 if the molecule is in the hydration layer, and it remains at 1 as long as the molecule stays in the hydration layer. It decays to 0 when the molecule leaves the hydration layer. The algorithms are described in detail elsewhere.[84-86]

Our calculations suggest water molecules occupy the first hydration layer longer than water molecules in the second hydration layer. This is due to the interactions between water molecules in the first hydration layer and calcite, as previously observed. In fact, most water molecules did not leave the first hydration layer during our analysis. Therefore, the residence time decays for water molecules in the second hydration layer are investigated in detail to reveal the effects of NaCl concentration, cation type and the force field applied. The results shown in Figure 15 and Figure 16 reveal complex trends perhaps represented by 2 timescales.

With the force field proposed by Xiao et al.,[44] at times less than ~ 14 ps, the rate of decay of $C_R(t)$ increases with NaCl concentration, indicating a smaller time constant as the NaCl concentration increases to 3 M. However, at times greater than ~ 14 ps, we observe slower $C_R(t)$ decay with increasing NaCl concentration. These results are consistent with those reported in the literature for the hydrogen bond dynamics of aqueous LiCl in the bulk.[7] Analysis of our results suggests that the decay curves of the corresponding residence autocorrelation functions can be fitted to the sum of two exponential decay equations by least squares fitting:[87]

$$C_R(t) = A_1 e^{\left(\frac{-t}{\tau_1}\right)} + A_2 e^{\left(\frac{-t}{\tau_2}\right)} \qquad (2)$$

In Eq. 2, τ_1 and τ_2 are decay constants, and A_1 and A_2 are coefficients, which were arbitrarily set to 0.5 assuming that the two decaying functions have equal weight on the auto-correlation function. The values of the fitted time constants are displayed in Table 5.

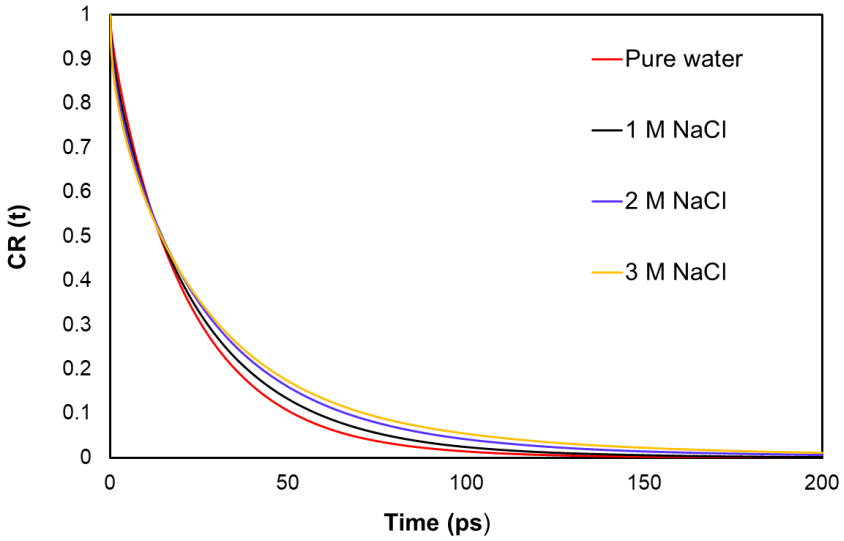

Figure 15. Residence autocorrelation functions $C_R(t)$ for oxygen atoms in the second hydration layer on the calcite surface. Results obtained for systems with pure water and 1 – 3 M NaCl. Results were obtained from simulations conducted using the force field proposed by Xiao et al.[44] to describe calcite. The simulations were conducted at 298 K.

In Figure 16, we analyse the effects of cations and that of the force field used to simulate calcite. The dynamics of water in 2 M NaCl and 2 M KCl are similar. For 2 M $MgCl_2$, at all times considered, the dynamics of water in the second hydration layer is slower than that for pure water. Compared to Na^+ and K^+, Mg^{2+} yields the slowest dynamics at times less than ~ 25 ps. However, after this time, water in $MgCl_2$ shows the fastest dynamics. $C_R(t)$ for water in the systems when the Raiteri et al.[45] force field was implemented show similar trends of bi-exponential decay with increased NaCl concentration, however it is characterized by faster decay than Xiao et al.[44] through the whole timeframe considered. It is worth noting that the force field using original parameters from Raiteri et al.[45] produce water with slower dynamics than in the implementation of LJ parameters from Shen et al.[46] We also computed the bi-exponential decay constants for these systems, which are reported in Table 5. The differences in residence times as predicted by the two force fields could be used to discriminate which of the two force fields yields more realistic results, but unfortunately the correspondent experimental data are not available.

Table 5. Time constants for bi-exponential fit for the residence autocorrelation function of water at 0-3 M NaCl, 2M KCl and 2M $MgCl_2$. The simulations were conducted at 298 K.

Salt Concentration	**τ_1 (ps)**	**τ_2 (ps)**
Pure Water	14.5	28.9
1 M NaCl	12.4	35.6
2 M NaCl	11.1	42.2
3 M NaCl	9.8	46.9
2 M KCl	11.1	42.5
2 M $MgCl_2$	15.6	34.1
Pure Water (Raiteri LJ)	6.5	12.1
2 M NaCl (Raiteri LJ)	4.6	22.4

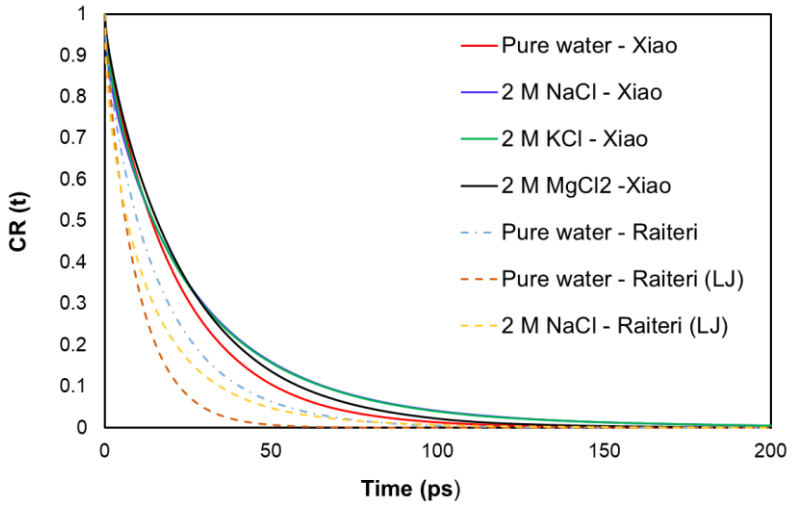

Figure 16. Residence autocorrelation functions $C_R(t)$ for oxygen atoms in the second hydration layer on calcite. Results obtained for systems with pure water, 2 M NaCl, 2 M KCl and 2 M $MgCl_2$ are compared. Solid lines represent results from simulations conducted using the force field proposed by Xiao et al.[44] Dashed lines represent the results from the implementation of the force field by Raiteri et al.[45] The simulations were conducted at 298 K.

4. CONCLUSIONS

Molecular dynamics simulations were conducted to investigate the role salts play on the interactions between calcite and interfacial water. In order to understand the structural properties of water for 0 – 3 M NaCl, 2 M KCl and 2 M $MgCl_2$, we determined atomic density profiles, surface density distributions, radial distribution functions, hydrogen bond networks, and orientation of interfacial water molecules. The dynamical properties of water were quantified in terms of the residence autocorrelation functions. Two force fields used to model calcite were compared for systems with pure water on the calcite surface. The results confirmed the formation of distinct hydration layers on the solid substrate. The addition of electrolytes had discernible effects on the surface density distributions, hydrogen bond network, and residence times, with the second hydration layer being affected more by the presence of salts than the first hydration layer. This could be due to the strong interactions between calcite and water, which make it more difficult for salts to perturb the first hydration layer. We found that the effects of the cations depend largely on the size of the cation. We also observed two timescales in the residence times of water molecules which we quantified with a bi-exponential model.

The hydration layers obtained from the implementation of the force field developed by Raiteri et al.[45] are closer to the surface, with slightly different orientation. The most significant difference in the two force fields is the residence times of water, with the force field proposed by Xiao et al.[44] yielding slower dynamics of interfacial water. In order to discriminate the most reliable among the two force fields, relevant experiments are required. X-ray reflectivity data

are available for the calcite-water interface[23,24,28] but they cannot identify the structure of hydrogen atoms, due to the small scattering cross-sectional area. However, X-ray reflectivity data are for the most part in agreement with the interfacial water structure predicted by both of the force fields implemented in this work. Neutron diffraction has a better sensitivity to hydrogen atoms. Other techniques such as Atomic Force Microscopy (AFM), and Infrared Spectroscopy (IR) can be used to identify the surface distribution, hydrogen bonding and orientation of water on mineral surfaces.[88,89] Sum Frequency Generation – Vibration Spectroscopy (SFG-VS) and Optical Second Harmonic Generation (SHG) are surface-sensitive techniques used to probe the structure interfacial molecules on solid/liquid interfaces. Nuclear Magnetic Resonance (NMR) spectroscopy, a fast, non-destructive technique, could also be used to probe the dynamics of water at solid-liquid interfaces.[90-95] The results presented here will provide a dataset on which to compare future experimental studies, towards the understanding of fundamental properties of relevance to large scale applications such as enhanced oil recovery or carbon sequestration.

ACKNOWLEDGEMENTS

We acknowledge the financial support from the U.S. Department of Energy, Office of Basic Energy Sciences, under Contract No. DE-SC0006878 (Division of Chemical Sciences, Geosciences, and Biosciences), Geosciences Program. Additional financial support was provided by the A. P. Sloan Foundation via the Deep Carbon Observatory administered by the Carnegie Institution for Science. AA was supported by the UK EPSRC Centre for Doctoral Training in the Advanced Characterisation of Materials (Grant No. EP/S023259/1). AS acknowledges financial support from the Science4CleanEnergy consortium (S4CE), which is supported by the Horizon2020 R&D programme of the European Commission, via grant No. 764810. Generous allocations of computing time were provided by the National Energy Research Scientific Computing Center (NERSC) at Lawrence Berkeley National Laboratory, Berkeley, CA. NERSC is supported by the DOE Office of Science. We are also grateful to the University College London Research Computing Platforms Support (MYRAID, GRACE and KATHLEEN) and the UK Materials and Molecular Modelling Hub (THOMAS), for access to high-performance computing.

SUPPORTING INFORMATION

Water density profiles along the Z direction at the various salt concentrations considered, in systems using the force field proposed by Xiao et al.[44]; density profiles of Na^+ ions in 2 M NaCl systems, surface density distributions of oxygen atoms in the second hydration layer of systems with no salts and 2 M NaCl, obtained from the force field proposed by Raiteri et al.[45]; oxygen - oxygen and Na^+ - oxygen radial distribution functions for systems with no salts and 2 M NaCl. This material is available free of charge at https://pubs.ac.org/doi/

REFERENCES

1. Chalbaud, C.; Robin, M.; Lombard, J.-M.; Martin, F.; Egermann, P.; Bertin, H., Interfacial Tension Measurements and Wettability Evaluation for Geological CO2 Storage. *Advances in Water Resources* **2009,** *32*, 98-109.
2. Lafitte, T.; Mendiboure, B.; Pineiro, M. M.; Bessieres, D.; Miqueu, C., Interfacial Properties of Water/CO2: A Comprehensive Description through a GradientTheory-SAFT-VR Mie Approach. *J Phys Chem* **2010,** *114*, 11110–11116.
3. Xing, W.; Song, Y.; Zhang, Y.; Nishio, M.; Zhan, Y.; Jian, W.; Shen, Y., Research Progress of the Interfacial Tension in Supercritical CO2-Water/Oil System. *Energy Procedia* **2013,** *37*, 6928-6935.
4. Mohammed, M.; Babadagli, T., Wettability Alteration: A comprehensive Review of Materials/Methods and Testing the Selected Ones on Heavy-Oil Containing Oil-Wet Systems. *Adv Colloid Interface Sci* **2015,** *220*, 54-77.
5. Leberman, R.; Soper, A. K., Effect of High Salt Concentrations on Water Structure. *Nature* **1995,** *378*, 364-366.
6. Smith, J. D.; Saykally, R. J.; Geissler, P. L., The Effects of Dissolved Halide Anions on Hydrogen Bonding in Liquid Water. *J Am Chem Soc* **2007,** *129*, 13847-13856.
7. Han, S., Dynamic Features of Water Molecules in Superconcentrated Aqueous Electrolytes. *Sci Rep* **2018,** *8*, 9347.
8. Laage, D.; Stirnemann, G., Effect of Ions on Water Dynamics in Dilute and Concentrated Aqeous Salt Solutions. *J Phys Chem B* **2019,** *125*, 3312-3324.
9. Hribar, B.; Southall, N. T.; Vlachy, V.; Dill, K. A., How Ions Affect the Structure of Water. *J Am Chem Soc* **2002,** *124*, 12302–12311.
10. Kanno, H.; Yonehama, K.; Somraj, A.; Yoshimura, Y., Structure-Making Ions Become Structure Breakers in Glassy Aqueous Electrolyte Solutions. *Chem Phy Lett* **2006,** *427*, 82-86.
11. Conte, P., Effects of Ions on Water Structure: a Low-Field ^{1}H T_1 NMR Relaxometry Approach. *Magn Reson Chem* **2015,** *53*, 711-718.
12. Nag, A.; Chakraborty, D.; Chandra, A., Effects of Ion Concentration on the Hydrogen Bonded Structure of Water in the Vicinity of Ions in Aqueous NaCl Solutions *J Chem Sci* **2008,** *120*, 71–77.
13. Riemenschneider, J.; Holzmann, J.; Ludwig, R., Salt Effects on the Structure of Water Probed by Attenuated Total Reflection Infrared Spectroscopy and Molecular Dynamics Simulations. *Chem Phys Chem* **2008,** *9*, 2731-2736.
14. Yoshida, K.; Ibuki, K.; Ueno, M., Estimated Ionic B-Coefficients from NMR Measurements in Aqueous Electrolyte Solutions *J Sol Chem* **1996,** *25*, 435–453.
15. Heberling, F.; Trainor, T. P.; Lützenkirchen, J.; Eng, P.; Denecke, M. A.; Bosbach, D., Structure and reactivity of the calcite–water interface. *J Colloid Interface Sci* **2011,** *354*, 843-857.
16. Argyris, D.; Ho, T.; Cole, D. R.; Striolo, A., Molecular Dynamics Studies of Interfacial Water at the Alumina Surface. *J Phys Chem C* **2011,** *115*, 2038-2046.
17. Argyris, D.; Tummala, N. R.; Striolo, A.; Cole, D. R., Molecular Structure and Dynamics in Thin Water Films at the Silica and Graphite Surfaces. *J Phys Chem C* **2008,** *112*, 13587-13599.
18. Ho, T. A.; Argyris, D.; Papavassiliou, D. V.; Striolo, A.; Lee, L. L.; Cole, D. R., Interfacial Water on Crystalline Silica: a Comparative Molecular Dynamics Simulation Study. *Mol Simulat* **2011,** *37*, 172-195.
19. Skelton, A. A.; Fenter, P.; Kubicki, J. D.; Wesolowski, D. J.; Cummings, P. T., Simulations of the Quartz$(10\bar{1}1)$/Water Interface: A Comparison of Classical Force Fields, Ab

Initio Molecular Dynamics, and X-ray Reflectivity Experiments. *J Phy Chem C* **2011,** *115*, 2076-2088.
20. Schlegel, M. L.; Nagy, K. L.; Fenter, P.; Sturchio, N. C., Structures of Quartz (100)- and (101)-Water Interfaces determined by X-ray Reflectivity and Atomic Force Microscopy of Natural Growth Surfaces. *Geochim Cosmochim Ac* **2002,** *66*, 3037-3054.
21. Malani, A.; Ayappa, K. G., Relaxation and Jump Dynamics of Water at the Mica Interface. *J Chem Phys* **2012,** *136*, 194701.
22. Wang, J.; Kalinichev, A. G.; Kirkpatrick, R. J.; Cygan, R. T., Structure, Energetics, and Dynamics of Water Adsorbed on the Muscovite (001) Surface: A Molecular Dynamics Simulation. *J Phys Chem B* **2005,** *109*, 15893-15905.
23. Fenter, P.; Kerisit, S.; Raiteri, P.; Gale, J. D., Is the Calcite–Water Interface Understood? Direct Comparisons of Molecular Dynamics Simulations with Specular X-ray Reflectivity Data. *J Phys Chem C* **2013,** *117*, 5028-5042.
24. Fenter, P.; Sturchio, N. C., Calcite (104)–Water Interface Structure, Revisited. *Geochim Cosmochim Acta* **2012,** *97*, 58-69.
25. Kerisit, S.; Parker, S. C., Free Energy of Adsorption of Water and Metal Ions on the {10$\bar{1}$4} Calcite Surface. *J Am Chem Soc* **2004,** *126*, 10152-10161.
26. Perry, T. D.; Cygan, R. T.; Mitchell, R., Molecular Models of a Hydrated Calcite Mineral Surface. *Geochim Cosmochim Acta* **2007,** *71*, 5876-5887.
27. Zhu, B.; Xu, X.; Tang, R., Hydration Layer Structures on Calcite Facets and Their Roles in Selective Adsorptions of Biomolecules: A Molecular Dynamics Study. *J Chem Phys* **2013,** *139*, 234705.
28. Fenter, P.; Geissbuhler, P.; DiMasi, E.; Srajer, G.; Sorensen, L. B.; Sturchio, N. C., Surface Speciation of Calcite Observed in Situ by High-Resolution X-Ray Reflectivity. *Geochim Cosmochim Ac* **2000,** *64*, 1221-1228.
29. Le, T. T. B.; Striolo, A.; Cole, D. R., Supercritical CO2 Effects on Calcite Wettability: A Molecular Perspective. *J Phys Chem C* **2020,** *124*, 18532–18543.
30. Ho, T. A.; Argyris, D.; Cole, D. R.; Striolo, A., Aqueous NaCl and CsCl Solutions Confined in Crystalline Slit-Shaped Silica Nanopores of Varying Degree of Protonation. *Langmuir* **2012,** *28*, 1256-1266.
31. Argyris, D.; Cole, D. R.; Striolo, A., Ion-Specific Effects under Confinement:The Role of Interfacial Water. *ACS Nano* **2010,** *4*, 2035-2042.
32. Ma, Y.-M.; Zhang, H.; Zhang, B.-J., Structure of Sodium Sulphate Aqueous Solution/Quartz Interface: A Molecular Dynamics Simulation. *Mol Simulat* **2014,** *40*, 634-639.
33. DelloStritto, M. J.; Kubicki, J. D.; Sofo, J. O., Effect of Ions on H-Bond Structure and Dynamics at the Quartz(101)–Water Interface. *Langmuir* **2016,** *32*, 11353-11365.
34. DelloStritto, M. J.; Kubicki, J.; Sofo, J. O., Density Functional Theory Simulation of Hydrogen-Bonding Structure and Vibrational Densities of States at the Quartz (1 0 1)-Water Interface and Its Relation to Dissolution as a Function of Solution pH and Ionic Strength. *J Phys: Condens Matter* **2014,** *26*, 244101.
35. Kerisit, S.; Ilton, E. S.; Parker, S. C., Molecular Dynamics Simulations of Electrolyte Solutions at the (100) Goethite Surface. *J Phys Chem B* **2006,** *110*, 20491-20501.
36. Simonnin, P.; Marry, V.; Noetinger, B.; Nieto-Draghi , C.; Rotenberg, B., Mineral- and Ion-Specific Effects at Clay–Water Interfaces: Structure, Diffusion, and Hydrodynamics. *J Phys Chem C* **2018,** *122*, 18484-18492.
37. Předota, M.; Bandura, A. V.; Cummings, P. T.; Kubicki, J. D.; Wesolowski, D. J.; Chialvo, A. A.; Machesky, M. L., Electric Double Layer at the Rutile (110) Surface. 1. Structure of Surfaces and Interfacial Water from Molecular Dynamics by Use of ab Initio Potentials. *J Phy Chem B* **2004,** *108*, 12049-12060.

38. Předota, M.; Zhang, Z.; Fenter, P.; Wesolowski, D. J.; Cummings, P. T., Electric Double Layer at the Rutile (110) Surface. 2. Adsorption of Ions from Molecular Dynamics and X-ray Experiments. *J Phy Chem B* **2004,** *108*, 12061-12072.
39. Zhang, Z.; Fenter, P.; Cheng, L.; Sturchio, N. C.; Bedzyk, M. J.; Machesky, M. L.; Anovitz, L. M.; Wesolowski, D. J., Zn2+ and Sr2+ adsorption at the TiO2 (110)–electrolyte interface: Influence of ionic strength, coverage, and anions. *J Colloid Interface Sci* **2006,** *295*, 50-64.
40. Zhang, Z.; Fenter, P.; Cheng, L.; Sturchio, N. C.; Bedzyk, M. J.; Předota, M.; Bandura, A.; Kubicki, J. D.; Lvov, S. N.; Cummings, P. T., et al., Ion Adsorption at the Rutile−Water Interface: Linking Molecular and Macroscopic Properties. *Langmuir* **2004,** *20*, 4954-4969.
41. Zhang, Z.; Fenter, P.; Kelly, S. D.; Catalano, J. G.; Bandura, A. V.; Kubicki, J. D.; Sofo, J. O.; Wesolowski, D. J.; Machesky, M. L.; Sturchio, N. C., et al., Structure of Hydrated Zn2+ at the Rutile TiO2 (110)-Aqueous Solution Interface: Comparison of X-ray Standing Wave, X-Ray Absorption Spectroscopy, and Density Functional Theory Results. *Geochim Cosmochim Ac* **2006,** *70*, 4039-4056.
42. Santos, M. S.; Castier, M.; Economou, I. G., Molecular Dynamics Simulation of Electrolyte Solutions Confined by Calcite Mesopores. *Fluid Phase Equilib* **2019,** *487*, 24−32.
43. Koleini, M. M.; Mehraban, M. F.; Ayatollahi, S., Effects of Low Salinity Water on Calcite/Brine Interface: A Molecular Dynamics Simulation Study. *Colloids Surf A* **2018,** *537*, 61–68.
44. Xiao, S.; Edwards, S. A.; Grater, F., A New Transferable Forcefield for Simulating the Mechanics of CaCO3 Crystals. *J Phys Chem C* **2011,** *115*, 20067-20075.
45. Raiteri, P.; Gale, J. D.; Quigley, D.; Rodger, P. M., Derivation of an Accurate Force-Field for Simulating the Growth of Calcium Carbonate from Aqueous Solution: A New Model for the Calcite−Water Interface. *J Phys Chem C* **2010,** *114*, 5997-6010.
46. Shen, J.-W.; Li, C.; van der Vegt, N. F. A.; Peter, C., Understanding the Control of Mineralization by Polyelectrolyte Additives: Simulation of Preferential Binding to Calcite Surfaces. *J Phys Chem C* **2013,** *117*, 6904-6913.
47. Berendsen, H. J. C.; Grigera, J. R.; Straatsma, T. P., The Missing Term in Effective Pair Potentials. *J Phys Chem* **1987,** *91*, 6269-6271.
48. Joung, I. S.; Cheatham, T. E., Determination of Alkali and Halide Monovalent Ion Parameters for Use in Explicitly Solvated Biomolecular Simulations. *J Phys Chem B* **2008,** *112*, 9020-9041.
49. Duboué-Dijon, E.; Mason, P. E.; Fischer, H. E.; Jungwirth, P., Hydration and Ion Pairing in Aqueous Mg2+ and Zn2+ Solutions: Force-Field Description Aided by Neutron Scattering Experiments and Ab Initio Molecular Dynamics Simulations. *J Phys Chem B* **2018,** *122*, 3296-3306.
50. Pluhařová, E.; Fischer, H. E.; Mason, P. E.; Jungwirth, P., Hydration of the Chloride Ion in Concentrated Aqueous Solutions using Neutron Scattering and Molecular Dynamics. *Mol Phys* **2014,** *112*, 1230-1240.
51. Pluhařová, E.; Mason, P. E.; Jungwirth, P., Ion Pairing in Aqueous Lithium Salt Solutions with Monovalent and Divalent Counter-Anions. *J Phys Chem A* **2013,** *117*, 11766-11773.
52. Kohagen, M.; Mason, P. E.; Jungwirth, P., Accurate Description of Calcium Solvation in Concentrated Aqueous Solutions. *J Phys Chem B* **2014,** *118*, 7902-7909.
53. Leontyev, I.; Stuchebrukhov, A., Accounting for Electronic Polarization in Non-Polarizable Force Fields. *Phys Chem Chem Phys* **2011,** *13*, 2613-2626.
54. Jorgensen, W. L.; Chandrasekhar, J.; Madura, J. D.; Impey, R. W.; Klein, M. L., Comparison of Simple Potential Functions for Simulating Liquid Water *J Chem Phys* **1983,** *79*, 926-935.

55. Harrach, M. F.; Drossel, B., Structure and Dynamics of TIP3P, TIP4P, and TIP5P Water Near Smooth and Atomistic Walls of Different Hydroaffinity. *J Chem Phys* **2014,** *140*, 174501.
56. Benavides, A. L.; Aragones, J. L.; Vega, C., Consensus on the Solubility of NaCl in Water from Computer Simulations using the Chemical Potential Route *J Chem Phys* **2016,** *144*, 124504.
57. Darden, T.; York, D. M.; Pedersen, L. G., Particle Mesh Ewald: An N·log(N) Method for Ewald Sums in Large Systems. *J Chem Phys* **1993,** *98*, 10089.
58. Allen, M. P.; Tildesley, D. J., *Computer Simulation of Liquids;* Oxford University Press: Oxford, UK, 2004.
59. Aragones, J. L.; Sanz, E.; Vega, C., Solubility of NaCl in Water by Molecular Simulation Revisited. *J Chem Phys* **2012,** *136*, 244508.
60. Joung, I. S.; Cheatham, T. E., Molecular Dynamics Simulations of the Dynamic and Energetic Properties of Alkali and Halide Ions Using Water-Model-Specific Ion Parameters. *J Phys Chem B* **2009,** *113*, 13279-13290.
61. Yagasaki, T.; Matsumoto, M.; Tanaka, H., Lennard-Jones Parameters Determined to Reproduce the Solubility of NaCl and KCl in SPC/E, TIP3P, and TIP4P/2005 Water. *J Chem Theory Comput* **2020,** *16*, 2460-2473.
62. Hess, B.; Kutzner, C.; van der Spoel, D.; Lindahl, E., GROMACS 4: Algorithms for Highly Efficient, Load-Balanced, and Scalable Molecular Simulation. *J Chem Theory Comput* **2008,** *4*, 435–447.
63. van der Spoel, D. L., E.; Hess, B.; Groenhof, G.; Mark, A. E.; Berendsen, H. J. C. , GROMACS: Fast, Flexible, and Free *J Comput Chem* **2005,** *26*, 1701–1718.
64. Plimpton, S., Fast Parallel Algorithms for Short-Range Molecular Dynamics *J Comput Phys* **1995,** *117*, 1-19.
65. Hoover, W. G., Canonical Dynamics : Equilibrium Phase-Space Distributions. *Phys Rev A* **1985,** *31*, 1695-1697.
66. Nose, S., A Molecular-Dynamics Method for Simulations in the Canonical Ensemble *Mol Phys* **1984,** *52*, 255-268.
67. Miyamoto, S.; Kollman, P. A., Settle: An Analytical Version of the SHAKE and RATTLE Algorithm for Rigid Water Models *J Comput Chem 13*, 952–962.
68. Marcus, Y., Effect of Ions on the Structure of Water: Structure Making and Breaking. *Chemical Reviews* **2009,** *109*, 1346-1370.
69. Soper, A. K., The Radial Distribution Functions of Water as Derived from Radiation Total Scattering Experiments: Is There Anything We Can Say for Sure? *ISRN Phys Chem* **2013**, 1-67.
70. Gurinaa, D. L.; Antipovab, M. L.; Petrenko, V. E., Radial Distribution Functions of Sub- and Supercritical Water According to the Nonempirical Molecular Dynamics Data. *Russ J Phys Chem* **2011,** *85*, 797-803.
71. Camisasca, G.; Pathak, H.; Wikfeldt, K. T.; Pettersson, L. G. M., Radial Distribution Functions of Water: Models vs Experiments. *J Chem Phys* **2019,** *151*, 004502.
72. Soper, A. K., The Radial Distribution Functions of Water and Ice from 220 to 673 K and at Pressures up to 400 MPa. *Chem Phys* **2000,** *258*, 121-137.
73. Rowley, C. N.; Roux, B., The Solvation Structure of Na+ and K+ in Liquid Water Determined from High Level ab Initio Molecular Dynamics Simulations. *J Chem Theory Comput* **2012,** *8*, 3526-3535.
74. Cassone, G.; Creazzo, F.; Giaquinta, P. V.; Saija, F.; Saitta, A. M., Ab Initio Molecular Dynamics Study of an Aqueous NaCl Solution under an Electric Field. *Phys Chem Chem Phys* **2016,** *18*, 23164-23173.

75. Aydin, F.; Zhan, C.; Ritt, C.; Epsztein, R.; Elimelech, M.; Schwegler, E.; Pham, T. A., Similarities and Differences between Potassium and Ammonium Ions in Liquid Water: a First-Principles Study. *Phys Chem Chem Phys* **2020,** *22*, 2540-2548.
76. Ikeda, T.; Boero, M.; Terakura, K., Hydration of Alkali Ions from First Principles Molecular Dynamics Revisited. *J Chem Phys* **2007,** *126*, 034501.
77. Hartkamp, R.; Coasne, B., Structure and Transport of Aqueous Electrolytes: From Simple Halides to Radionuclide ions. *J Chem Phys* **2014,** *141*, 124508.
78. Zapałowski, M.; Bartczak, W. M., Concentrated Aqueous $MgCl_2$ Solutions. A Computer Simulation Study of the Solution Structure and Excess Electron Localisation. *Res Chem Intermed* **2001,** *27*, 855-866.
79. Dietz, W.; Riede, W. O.; Heinzinger, K., Molecular Dynamics Simulation of an Aqueous MgCl2 Solution. Structural Results. *Zeitschrift für Naturforschung A* **1982,** *37*, 1038-1048.
80. Marti, J., Analysis of the Hydrogen Bonding and Vibrational Spectra of Supercritical Model Water by Molecular Dynamics Simulations. *J Chem Phys* **1999,** *110*, 6876-6886.
81. Di Tommaso, D.; Ruiz-Agudo, E.; de Leeuw, N. H.; Putnis, A.; Putnis, C. V., Modelling the Effects of Salt Solutions on the Hydration of Calcium Ions. *Phys Chem Chem Phys* **2014,** *16*, 7772-7785.
82. Wolthers, M.; Di Tommaso, D.; Du, Z.; de Leeuw, N. H., Calcite Surface Structure and Reactivity: Molecular Dynamics Simulations and Macroscopic Surface Modelling of the Calcite–Water Interface. *Phys Chem Chem Phys* **2012,** *14*, 15145-15157.
83. Soper, A. K.; Bruni, F.; Ricci, M. A., Site–site Pair Correlation Functions of Water from 25 to 400 °C: Revised Analysis of New and Old Diffraction data. *J Chem Phys* **1997,** *106*, 247-254.
84. Argyris, D.; Cole, D. R.; Striolo, A., Dynamic Behavior of Interfacial Water at the Silica Surface *J Phys Chem C* **2009,** *113*, 19591-19600.
85. Ho, T. A.; Striolo, A., Polarizability Effects in Molecular Dynamics Simulations of the Graphene-Water Interface. *J Chem Phys* **2013,** *138*, 054117.
86. Phan, A.; Cole, D. R.; Striolo, A., Preferential Adsorption from Liquid Water–Ethanol Mixtures in Alumina Pores. *Langmuir* **2014,** *30*, 8066-8077.
87. Debnath, A.; Mukherjee, B.; Ayappa, K. G.; Maiti, P. K.; Lin, S.-T., Entropy and Dynamics of Water in Hydration Layers of a Bilayer *J Chem Phys* **2010,** *133*, 17404.
88. Verdaguer, A.; Sacha, G. M.; Bluhm, H.; Salmeron, M., Molecular Structure of Water at Interfaces: Wetting at the Nanometer Scale. *Chem Rev* **2006,** *106*, 1478-1510.
89. Näslund, L. Å.; Lüning, J.; Ufuktepe, Y.; Ogasawara, H.; Wernet, P.; Bergmann, U.; Pettersson, L. G. M.; Nilsson, A., X-ray Absorption Spectroscopy Measurements of Liquid Water. *J Phys Chem B* **2005,** *109*, 13835-13839.
90. Blicharska, B.; Peemoeller, H.; Witek, M., Hydration Water Dynamics In Biopolymers From NMR Relaxation in the Rotating Frame. *J Mag Res* **2010,** *207*, 287-293.
91. Chen, Y.-W.; Hseih, C.-J.; Lin, C.-M.; Hwang, D. W., NMR Relaxation Study of Water Dynamics in Superparamagnetic Iron-Oxide-Loaded Vesicles. *J Chem Phys* **2013,** *138*, 064502.
92. Lusceac, S. A.; Vogel, M., ^{2}H NMR Study of the Water Dynamics in Hydrated Myoglobin. *J Phys Chem B* **2010,** *114*, 10209–10216.
93. Schneider, S.; Vogel, M., NMR Studies on The Coupling of Ion and Water Dynamics on Various Time and Length Scales in Glass-Forming LiCl Aqueous Solutions. *J Chem Phys* **2018,** *149*, 104501.
94. Traore, A.; Foucat, L.; Renou, J. P., ^{1}H-NMR Study of Water Dynamics in Hydrated Collagen: Transverse Relaxation-Time and Diffusion Analysis *Bioploymers* **2000,** *53*, 476-483.

95. Weigler, M.; Brodrecht, M.; Breitzke, H.; Dietrich, F.; Sattig, M.; Buntkowsky, G.; Vogel, M., ^{2}H NMR Studies on Water Dynamics in Functionalized Mesoporous Silica. *Z Phys Chem* **2018,** *232*, 1041.

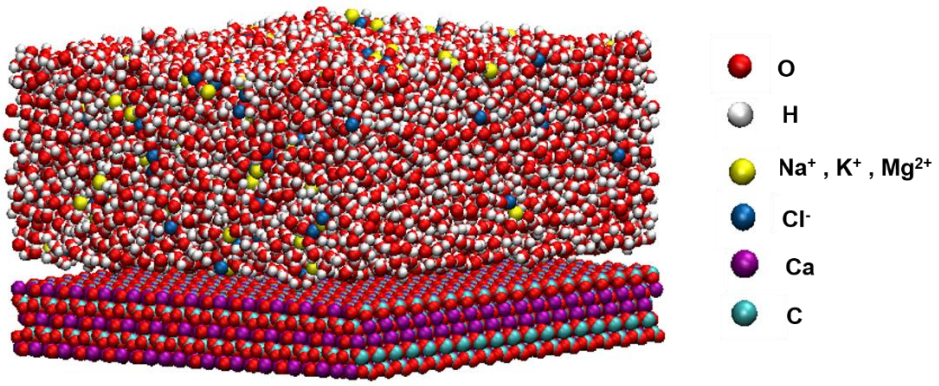

TOC Graphic